

DRAFT

IMECE2016-66470

NONLINEAR STABILITY ANALYSIS OF A MACROSCOPIC TRAFFIC FLOW MODEL FOR ADAPTIVE CRUISE CONTROL SYSTEMS

Kallirroi N. Porfyri, Ioannis K. Nikolos¹, Anargiros I. Delis, Markos Papageorgiou
Technical University of Crete, School of Production Engineering and Management
University Campus, GR-73100, Chania, Greece

¹Contact Author

ABSTRACT

The occurrence of perturbations in traffic flow may lead to the formation of stop-and-go waves traveling upstream, or to traffic jams. Therefore, traffic flow stability analysis is considered to be one of the fundamental problems in traffic flow theory, and a lot of effort has been spent to analyze the formation and evolution of such traffic flow instabilities. Recent advances in the field of Vehicle Automation and Communication Systems (VACS), such as Adaptive Cruise Control (ACC) systems, are a potential remedy to reduce the magnitude or even to eradicate the formation of such traffic flow instabilities. To this end, this work aims to perform a nonlinear stability analysis of a second-order macroscopic traffic flow model, recently developed by the authors, to simulate the flow of ACC-equipped vehicles and identify the ways that ACC systems influence the stability of traffic flow, in relation with large traffic disturbances around the equilibrium state. Numerical simulations are additionally conducted, to verify the derived stability condition.

Keywords: Nonlinear stability analysis, macroscopic traffic flow modeling, Adaptive Cruise Control.

1. INTRODUCTION

The frequent occurrence of perturbations in traffic flow, such as sudden deceleration of vehicles, or the non-uniformity of the flow entering a highway from an on-ramp, may, under circumstances, lead to stop-and-go waves traveling upstream, or traffic jams, resulting in considerable time-delays, increased fuel consumption and air pollution, as well as a serious under-utilization of the available infrastructure. Consequently, traffic flow stability analysis is considered to be one of the fundamental tools in traffic flow theory, and scientists have been particularly interested in understanding the formation and evolution of such traffic flow instabilities since the early days of traffic engineering. In general, there are two main modeling

approaches taken to predict traffic flow instabilities, the microscopic and macroscopic. The microscopic approach describes traffic flow behaviors at a high level of detail by capturing the behavior of each individual vehicle [1-4], while the macroscopic approach represents traffic in lesser detail by using aggregated variables, such as flow, density and mean speed [5-8].

Recent developments in the fields of Intelligent Transportation Systems (ITS) and Vehicle Automation and Communication Systems (VACS), such as Adaptive Cruise Control (ACC) systems, besides their contribution to safety and convenience of the passengers, are believed to be a potential remedy to the aforementioned traffic flow problems by reducing the effects of traffic flow instabilities with the appropriate selection of their operation parameters. This advanced feature, in conjunction with the expected extensive use of such systems in the near future, can provide additional tools for the mitigation of the rapidly growing problem of traffic congestion.

In principle, the ACC systems, which are already commercially available in the passenger car market, allow vehicles to follow their preceding vehicle automatically, by controlling the throttle and the brake activations. More specifically, using a forward-looking range sensor, the ACC systems are able to estimate the time gap to the vehicle immediately in front of them -referred to as the leader-, the speed difference, as well as the speed of the equipped vehicle. Hence, in cases that the leader drives at lower speed, the ACC-equipped vehicle slows down to realize a desired time-gap, while, on the other hand, in cases that the leader either accelerates or is out of the range of the ACC vehicle's sensors, the equipped vehicle accelerates towards and maintains a pre-set desired speed. ACC systems have been focused on increasing driving comfort and safety, by relieving the driver from continuous speed and time-gap adjustments; however, for particular selection of their operation parameters, they may

have negative consequences on the traffic flow performance and stability. Hence, research is focused on the development of effective (theoretical and numerical simulation) models for traffic flow including ACC-equipped vehicles, to provide tools for the evaluation of their effects on the traffic flow stability and efficiency. However, a significant query regarding the applicability of such tools is whether they are capable of reproducing the mechanisms leading to stop-and-go waves and traffic jams with the appearance of perturbations in traffic flow. If this is true, then those tools can be used for identifying the crucial parameters of ACC systems that result in a stable or unstable response to disturbances.

Many different approaches have been reported relying on microscopic traffic flow representation, either using microscopic simulation for the vehicle behavior in the presence of ACC systems, or using analytic approaches for the derivation of linear or nonlinear methods for predicting the growth of traffic flow instabilities; we refer for example to [9-18]. On the other hand, the corresponding literature pertaining to macroscopic or gas-kinetic traffic flow models is relatively limited [19-23]. It is worth mentioning here that the stability analysis using macroscopic models is referred as flow stability, while the string stability of a platoon of vehicles is obtained from microscopic approaches [20, 24]. However, concerning the models applicability, macroscopic traffic flow models call for much less computational demand than their microscopic counterparts and require simpler calibration and validation effort; hence, the development of such models for the simulation of ACC traffic will be of major significance in the future.

Towards this direction, this work attempts to perform a nonlinear stability analysis of a second-order macroscopic traffic flow model, which was recently developed by the authors to simulate the flow of ACC-equipped vehicles [25], and identify the ways that ACC systems influence the stability of traffic flow, in relation with large traffic flow disturbances around an equilibrium state; the proposed model has been developed on the grounds of the gas-kinetic-based traffic flow (GKT) model, by proper adaptations to take into account the effect of ACC (or CACC) vehicles. Numerical simulations are also performed to support the findings of the analytic procedure.

2. THE GKT MODEL FOR ACC SYSTEMS

In this section we recall the recently developed second-order macroscopic traffic flow model incorporating the behavior of ACC-equipped vehicles. The model has been developed based on the gas-kinetic traffic flow concept, which was first established in the '60s by Prigogine and Andrews [26]. During the last years, the concept has attracted increasing interest, by applying it to develop continuum macroscopic traffic flow models, as the GKT one [27-29], used also to derive variants for cooperative and ACC traffic flow [23, 30]. In particular, the aggregated traffic flow variables are obtained from microscopic level with explicit consideration of vehicle-driver dynamics, bridging in this way the gap between the

microscopic behavior of individuals and the macroscopic traffic flow dynamics. The new macroscopic traffic flow equations are derived from the gas-kinetic ones by means of the so-called method of moments [23, 28, 31-34]. It is worth mentioning that the arising partial differential equations in the GKT model and its variants, in contrast to other macroscopic traffic flow models, incorporate a non-local interaction term instead of a diffusion or viscosity one, which has beneficial properties concerning the rapidity and the robustness of numerical integration methods. Therefore, the GKT model provides the means for robust applications in cases of extended freeway networks that can be simulated in reasonable computational times [25, 35]. Moreover, the non-local GKT model is capable of simulating the hysteretic phase transitions to congested traffic with high traffic flow, the so-called "synchronized traffic", which is the most common form of congested states, typically occurring behind on-ramps, gradients, or other bottlenecks of busy highways [36, 37].

In the remainder of this section, we recast the GKT model, which was extended to incorporate the behavior of ACC vehicles. Let $\rho(x, t)$ denote the traffic density (number of vehicles per unit length) as a function in space, x , and time, t ; $u(x, t)$ the average speed of vehicles; while the traffic flow rate (number of vehicles per unit of time) is given as $q(\rho, u) = \rho(x, t)u(x, t)$. The modified GKT model in conservation law form is written as [25]

$$\partial_t(\rho) + \partial_x(\rho u) = 0, \quad (1)$$

$$\begin{aligned} \partial_t(\rho u) + \partial_x(\rho u^2 + \theta \rho) = \\ \rho \left(\frac{V_e^* - u}{\tau} \right) [1 - pF(\rho)] + pV_{acc} \end{aligned} \quad (2)$$

where Equation (1) reflects the conservation of vehicles. In the momentum dynamics Equation (2), the modeling of ACC vehicles has been integrated in the terms of pV_{acc} and $[1 - pF(\rho)]$ and will be explained subsequently, while for $p = 0$ the manual driving is modeled, as the original GKT model describes. The pressure-like term θ is a density-dependent fraction $A(\rho)$ of the squared velocity, $\theta = A(\rho)u^2$, where $A(\rho)$ is given by the Fermi function as:

$$A(\rho) = A_0 + \delta A \left[1 + \tanh \left(\frac{\rho - \rho_{cr}}{\delta \rho} \right) \right] \quad (3)$$

in which ρ_{cr} is the critical density, reflecting the boundary for the transition from the free flow to congested traffic and $\delta \rho$ is the width of the transition region. Typical range of values for the constants $\delta \rho$, A_0 , and δA are given in Table 1, along with other typical used model parameters for the GKT model, taking into account [23-25, 28, 29, 35].

Moreover, the momentum Equation (2) includes a traffic relaxation term to maintain the concentration of velocity in equilibrium state, with $V_e^*(\rho, u, \rho_\alpha, u_\alpha)$ being the dynamic

equilibrium speed that depends both on the local (ρ, u) and the non-local traffic state (ρ_α, u_α) , determined as

$$V_e^*(\rho, u, \rho_\alpha, u_\alpha) = u_{max} \left[1 - \frac{\theta + \theta_\alpha}{2A(\rho_{max})} \left(\frac{\rho_\alpha T}{1 - \rho_\alpha / \rho_{max}} \right)^2 B(\delta u) \right]. \quad (4)$$

According to Equation (4), the dynamic equilibrium speed is computed as the maximum desired speed, denoted as u_{max} , minus a braking non-local term in response to necessary deceleration maneuvers in traffic flow downstream, at the interaction location $x_\alpha = x + \gamma(1/\rho_{max} + T \cdot u)$, with T being the desired time-gap, ρ_{max} the maximum density and γ a scale parameter. Finally, the Boltzmann (interaction) factor B that contains the standard normal distribution and the Gaussian error function, is given as

$$B(\delta u) = 2 \left[\delta u \frac{e^{-\delta u^2/2}}{\sqrt{2\pi}} + (1 + \delta u^2) \int_{-\infty}^{\delta u} \frac{e^{-y^2/2}}{\sqrt{2\pi}} dy \right]. \quad (5)$$

This term describes the dependence of the braking interaction on the dimensionless velocity difference δu , with $\delta u = \frac{u - u_\alpha}{\sqrt{\theta + \theta_\alpha}}$, taking into account the velocity and variance at the actual position x and the anticipation location x_α .

The major difference compared to other macroscopic traffic flow models is the additional property of the GKT model to take into consideration the nonlocal interaction term in the equilibrium velocity (Equation (4)). This nonlocality has smoothing attributes similar to those of a diffusion or viscosity term, but its effect is more realistic as it is forwardly directed, which means that vehicles react on density or velocity gradients in front of them [28]. Moreover, in contrast to other macroscopic traffic flow models, the steady-state (equilibrium) speed-density relation of GKT model, $V^e(\rho)$, is not explicitly given, but results from the steady-state condition on homogeneous roads as

$$V^e(\rho) = \frac{\tilde{u}^2}{2u_{max}} \left(-1 + \sqrt{1 + \frac{4u_{max}^2}{\tilde{u}^2}} \right) \quad (6)$$

where the following abbreviation was used

$$\tilde{u} = \frac{1}{T} \left(\frac{1}{\rho} - \frac{1}{\rho_{max}} \right) \sqrt{\frac{A(\rho_{max})}{A(\rho)}}. \quad (7)$$

Subsequently, the developed modified model for the macroscopic simulation of ACC traffic was incorporated as a source term to the momentum equation of the GKT model, which controls the speed dynamics, contributing to the relaxation term in the GKT model equations and also taking

explicitly into account the important for ACC systems time-gap parameter; this is done through the terms pV_{acc} and $[1 - pF(\rho)]$ in Equation (2), where by setting $p = 1$ the ACC approach is obtained, while for $p = 0$ the GKT model equations for manual driving are modeled, as the original GKT model describes. A properly defined Fermi function $F(\rho)$ is used for the smooth transition between the two source terms corresponding to manual and ACC traffic, as it will be later explained.

Parameters	Units	Typical values
Desired free speed, u_{max}	km/h	[110,130]
Maximum density, ρ_{max}	veh/km	[140,160]
Critical density, ρ_{cr}	veh/km	[0.25, 0.4] ρ_{max}
Desired time gap, T	s	[1, 2]
Anticipation factor, γ		[1, 2]
Relaxation time, τ	s	[20, 40]
Variance pre-factor for free traffic, A_0		0.008
Pre-factor δA		$2.5A_0$
Transition width $\delta\rho$	veh/km	[0.05, 0.1] ρ_{max}

Tab. 1: Typical range of the parameters used for the GKT model

Next, it is essential to highlight the necessary control objectives that the ACC systems should follow, and which are adopted by the proposed approach, according to [38]:

- *Speed control mode:* to keep the vehicle velocity close to the maximum velocity pre-set by the user, in cases that the range of sensor systems (such as radar or lidar) do not detect leading vehicles, or leading vehicles are detected but their velocities are higher than the pre-set maximum velocity.
- *Gap control mode:* to retain vehicle velocity equal to the velocity of the leading vehicle in order to maintain the specified desired gap, in cases that the leading vehicle is identified by the sensor systems and its velocity is lower than the user-set maximum one.
- Transitions between the two aforementioned control modes are important to be smooth, so as to eliminate inconvenience to the passengers, on account of sudden changes of velocity or abrupt maneuvers.

We define *time/space-headway* as the time/space interval between the front bumpers of consecutive vehicles, while *time/space-gap* as the time/space interval between the rear bumper of the leading vehicle and the front bumper of the following one [24]. The most popular ACC policy is the Constant Time-Headway (CTH) one, adopted in the proposed modeling, where the inter-vehicle spacing is a linear function of the vehicle's speed [39]; consequently, the developed model is based on the following assumptions in order to implement the aforementioned objectives:

- I. In cases where the density is less than a threshold ρ_{acc} (which is lower than or equal to the critical density ρ_{cr}), there is limited or no influence of the

additional term to the GKT model. For density values around ρ_{acc} , a smooth but fast transition between the manual case and the ACC model is established, using the following Fermi function:

$$F(\rho) = \frac{1}{2} \left[1 + \tanh \left(\frac{\rho - \rho_{acc}}{\Delta\rho} \right) \right] \quad (8)$$

- II. In cases where the gap control mode is activated, the desired constant time gap T^* is imposed through its corresponding influence on a desired density ρ^* , given as [25]:

$$\rho^* = \frac{1}{1/\rho_{max} + T^*u^*} \quad (9)$$

The denominator in equation above reflects the desired space headway, with $1/\rho_{max}$ being the vehicle's length and $u^* = u(x^*)$ being the speed of the leading vehicle, computed at the "interaction" position [25]:

$$x^* = x + \gamma^*(1/\rho_{max} + T^* \cdot u), \quad \gamma^* \in [1, 2]. \quad (10)$$

In addition, using a relaxation time τ^* , the desired speed relaxes to the speed of the leading vehicle u^* . Accordingly, the corresponding source term of Equation (2) that reflects the behavior of ACC-equipped vehicles can be expressed as [25]

$$\begin{aligned} V_{acc}(\rho, u, \rho^*, u^*) &= \\ \frac{1}{2} \left[1 + \tanh \left(\frac{\rho - \rho_{acc}}{\Delta\rho} \right) \right] \left(\frac{\rho^*u^* - \rho u}{\tau^*} \right) & \quad (11) \\ = F(\rho) \left(\frac{\rho^*u^* - \rho u}{\tau^*} \right) & \end{aligned}$$

In [ISO 15622, 2010], it is recommended that for ACC systems the indicated values should be $T^* \in [0.8, 2.2]$ s, while τ^* is in the order of 1 s.

3. NONLINEAR STABILITY ANALYSIS FOR ACC SYSTEMS

The stability analysis method is a well-established technique for studying the ability of traffic flow models to describe the effects of traffic flow perturbations, such as accidents and other related phenomena, to traffic flow instability; its applicability is of essential importance, regarding the improvement of traffic flow capacity and efficiency as well as to ensure safe driving. Inherently, this approach concerns the study of solutions of a dynamical system in relation with small or higher introduced perturbations in the initial conditions. Indeed, in traffic flow theory, the response of drivers to a sudden stimulus, or to sudden spontaneous acceleration and deceleration, may result in the formation of disturbances that, in congested states, will eventually grow and will give rise to "phantom traffic jams" propagating upstream, against the traffic

flow. Hence, it is of significance to define the conditions under which the traffic state in case of macroscopic ones remain stable under a properly introduced perturbation [24].

Within the vast literature on macroscopic traffic flow modeling, both linear and nonlinear stability methods have been applied in order to derive stability criteria [3, 5, 7, 8, 19, 22-24, 30-32, 40-43]. At this point, it is important to highlight the difference between small and large perturbations in the stability analysis of traffic systems. Although there is a large body of research that deals with linearized methods to investigate traffic flow stability criteria by assuming that the perturbations are small, such approximate linearized stability methods neglect higher-order terms and are only applicable when the magnitude of perturbations is fairly small. Thus, since the linear stability method, recently developed by the authors for the proposed macroscopic model [44], is only valid for small disturbances, the nonlinear technique is followed in this work, as it allows to more accurately examine the global stability conditions under which a large perturbation travels against the traffic flow.

In this work, a nonlinear stability criterion is derived, using a wavefront expansion method under large perturbations, which enables to investigate the shock wave propagation properties of the developed ACC model [19, 22, 32, 45]. In principle, considering a perturbation that starts at a specific location x_0 in the stationary and spatially homogeneous (i.e. time- and space-independent) traffic state, (ρ_0, u_0) , of the traffic system, the wavefront is the propagation curve of such perturbation along the homogenous (equilibrium) traffic flow. If the magnitude of the initial perturbation is not growing during its propagation, the traffic flow is nonlinearly stable. Conversely, if the amplitude of the perturbation is increased as it propagates against the traffic flow, traffic will become unstable, resulting in the formation of a shock wave or bottleneck on the highway.

Let us start with finding the unstable traffic regions through the wavefront expansion method of the proposed model, as described in the remainder of this section, taking primarily into account only the case of ACC-equipped vehicles (assuming that the flow is congested (thus the value of $F(\rho) \rightarrow 1$ in Equation (11)) and only the ACC-term is activated in the source term of Equation (2)). Therefore, Equations (1) and (2) are simplified in the following form:

$$\partial_t(\rho) + u\partial_x(\rho) + \rho\partial_x(u) = 0, \quad (12)$$

$$\begin{aligned} \partial_t(u) + u\partial_x(u) + \frac{1}{\rho} \left(\partial_\rho(P)\partial_x(\rho) + \partial_u(P)\partial_x(u) \right) &= \\ \frac{1}{\rho} \left(\frac{\rho^*u^* - \rho u}{\tau^*} \right) & \quad (13) \end{aligned}$$

where the abbreviations for partial derivatives are defined as:

$$\partial_t(\rho) = \frac{\partial\rho}{\partial t}, \quad \partial_t(u) = \frac{\partial u}{\partial t}, \quad \partial_x(\rho) = \frac{\partial\rho}{\partial x}, \quad (14)$$

$$\partial_x(u) = \frac{\partial u}{\partial x}, \quad \partial_\rho(P) = \frac{\partial P}{\partial \rho}, \quad \partial_u(P) = \frac{\partial P}{\partial u}.$$

To derive traffic flow propagation stability, we first need to expand the macroscopic traffic flow variables, such as density $\rho(x, t)$ and average speed $u(x, t)$, as well as the time and space partial derivatives of density and average speed downstream the wavefront in a power series of

$$\xi = x - X(t), \quad (15)$$

where $X(t)$ is the location of the wavefront at time instant t . Inherently, the wavefront complies with the characteristic velocity u_c , which will be derived later, at the equilibrium states, i.e.

$$\dot{X}(t) = \frac{dX}{dt} = u_0 + u_c. \quad (16)$$

Thus, using Equation (15), the aforementioned traffic flow variables are expanded in a power series of ξ as

$$\rho(x, t) = \rho_0 + \xi \partial_x(\rho(t)) + \frac{1}{2} \xi^2 \partial_{xx}(\rho(t)) + \dots \quad (17)$$

$$u(x, t) = u_0 + \xi \partial_x(u(t)) + \frac{1}{2} \xi^2 \partial_{xx}(u(t)) + \dots \quad (18)$$

$$\begin{aligned} \partial_t(\rho) = & -\dot{X}(t) \partial_x(\rho(t)) + \xi \dot{\rho}_x(t) \\ & + \xi \left(-\dot{X}(t) \partial_{xx}(\rho(t)) \right) + \\ & \frac{1}{2} \xi^2 \dot{\rho}_{xx}(t) + \dots \end{aligned} \quad (19)$$

$$\begin{aligned} \partial_t(u) = & -\dot{X}(t) \partial_x(u(t)) + \xi \dot{u}_x(t) \\ & + \xi \left(-\dot{X}(t) \partial_{xx}(u(t)) \right) + \\ & \frac{1}{2} \xi^2 \dot{u}_{xx}(t) + \dots \end{aligned} \quad (20)$$

$$\partial_x(\rho) = \partial_x(\rho(t)) + \xi \partial_{xx}(\rho(t)) + \frac{1}{2} \xi^2 \partial_{xxx}(\rho(t)) + \dots \quad (21)$$

$$\partial_x(u) = \partial_x(u(t)) + \xi \partial_{xx}(u(t)) + \frac{1}{2} \xi^2 \partial_{xxx}(u(t)) + \dots, \quad (22)$$

where

$$\begin{aligned} \dot{\rho}_x(t) &= \frac{d(\partial_x(\rho(t)))}{dt}, & \dot{u}_x(t) &= \frac{d(\partial_x(u(t)))}{dt}, \\ \dot{\rho}_{xx}(t) &= \frac{d(\partial_{xx}(\rho(t)))}{dt}, & \dot{u}_{xx}(t) &= \frac{d(\partial_{xx}(u(t)))}{dt}, \end{aligned} \quad (23)$$

$$\begin{aligned} \partial_x(\rho(t)) &= \frac{\partial \rho}{\partial x} \Big|_{X(t),t}, & \partial_x(u(t)) &= \frac{\partial u}{\partial x} \Big|_{X(t),t}, \\ \partial_{xx}(\rho(t)) &= \frac{\partial^2 \rho}{\partial x^2} \Big|_{X(t),t}, & \partial_{xx}(u(t)) &= \frac{\partial^2 u}{\partial x^2} \Big|_{X(t),t}, \\ \partial_{xxx}(\rho(t)) &= \frac{\partial^3 \rho}{\partial x^3} \Big|_{X(t),t}, & \partial_{xxx}(u(t)) &= \frac{\partial^3 u}{\partial x^3} \Big|_{X(t),t}. \end{aligned}$$

Similarly, expanding the derivatives of traffic pressure in relation with the local density and speed, as well as the desired density ρ^* and speed u^* of the preceding vehicle, we obtain

$$\partial_\rho(P) = \partial_\rho(P_0) + \xi(\partial_{\rho\rho}(P_0) \partial_x(\rho(t)) + \partial_{\rho u}(P_0) \partial_x(u(t))) + \dots \quad (24)$$

$$\partial_u(P) = \partial_u(P_0) + \xi(\partial_{u\rho}(P_0) \partial_x(\rho(t)) + \partial_{uu}(P_0) \partial_x(u(t))) + \dots \quad (25)$$

$$\rho^* = \rho_0 + \xi \partial_x(\rho(t)) + d^* (\partial_x(\rho(t)) + \xi \partial_{xx}(\rho(t))) + \dots \quad (26)$$

$$u^* = u_0 + \xi \partial_x(u(t)) + d^* (\partial_x(u(t)) + \xi \partial_{xx}(u(t))) + \dots, \quad (27)$$

where $d^* = x^* - x$, $P_0 = P(\rho_0, u_0)$, and

$$\begin{aligned} \partial_\rho(P_0) &= \frac{\partial P}{\partial \rho} \Big|_{X(t),t}, & \partial_{\rho\rho}(P_0) &= \frac{\partial^2 P}{\partial \rho^2} \Big|_{X(t),t}, \\ \partial_u(P_0) &= \frac{\partial P}{\partial u} \Big|_{X(t),t}, & \partial_{uu}(P_0) &= \frac{\partial^2 P}{\partial u^2} \Big|_{X(t),t}, \\ \partial_{\rho u}(P_0) &= \frac{\partial^2 P}{\partial \rho \partial u} \Big|_{X(t),t}, & \partial_{u\rho}(P_0) &= \frac{\partial^2 P}{\partial \rho \partial u} \Big|_{X(t),t}. \end{aligned} \quad (28)$$

Thereafter, we substitute Equations (17)-(28) into the system of Equations (12) and (13) and we produce two sets of equations, one for the original position (ξ^0) (for $\xi = 0$) and one for the perturbed position (ξ^1), taking also into account Equation (16). Thus, for the conservation Equation (12), we obtain the following expressions:

$$\xi^0 : -\partial_x(\rho) u_c + \rho_0 \partial_x(u) = 0, \quad (29)$$

$$\xi^1 : \dot{\rho}_x - \partial_{xx}(\rho) u_c + 2\partial_x(\rho) \partial_x(u) + \rho_0 \partial_{xx}(u) = 0. \quad (30)$$

Similarly, the momentum dynamics Equation (13) results in:

$$\begin{aligned} \xi^0 : & -u_c \partial_x(u) + \frac{1}{\rho_0} (\partial_\rho(P_0) \partial_x(\rho) + \partial_u(P_0) \partial_x(u)) = \\ & \frac{1}{\rho_0} \frac{1}{\tau^*} d^* (\rho_0 \partial_x(u) + u_0 \partial_x(\rho)), \end{aligned} \quad (31)$$

$$\begin{aligned} \xi^1 : \dot{u}_x - u_c \partial_{xx}(u) + (\partial_x(u))^2 - u_c \frac{\partial_x(\rho)}{\rho_0} \partial_x(u) + \\ \frac{1}{\rho_0} \partial_\rho(P_0) \partial_{xx}(\rho) + \frac{1}{\rho_0} \partial_{\rho\rho}(P_0) (\partial_x(\rho))^2 \\ + \frac{1}{\rho_0} \partial_{\rho u}(P_0) \partial_x(\rho) \partial_x(u) + \\ \frac{1}{\rho_0} \partial_u(P_0) \partial_{xx}(u) + \frac{1}{\rho_0} \partial_{u\rho}(P_0) \partial_x(\rho) \partial_x(u) = \\ \frac{1}{\tau^*} \left(d^* \partial_{xx}(u) + \frac{2}{\rho_0} d^* \partial_x(\rho) \partial_x(u) + \frac{1}{\rho_0} d^* u_0 \partial_{xx}(\rho) \right). \end{aligned} \quad (32)$$

Equation (29) yields to:

$$\partial_x(\rho) = \frac{\rho_0 \partial_x(u)}{u_c}. \quad (33)$$

Thus, substitution of Equation (33) into Equation (31) results in

$$u_c^2 - \left(\frac{1}{\rho_0} \partial_u(P_0) - \frac{1}{\tau^*} d^* \right) u_c + \frac{1}{\tau^*} d^* u_0 - \partial_\rho(P_0) = 0. \quad (34)$$

The solutions of the expression above are the characteristic velocities u_c , given as

$$u_{c\pm} = \frac{1}{2} \left(\frac{1}{\rho_0} \partial_u(P_0) - \frac{1}{\tau^*} d^* \right) \pm \sqrt{\left(\frac{1}{2\rho_0} \partial_u(P_0) - \frac{1}{2\tau^*} d^* \right)^2 + \partial_\rho(P_0) - \frac{1}{\tau^*} d^* u_0}. \quad (35)$$

In practice, under free flow conditions, where traffic demand is low enough, the perturbations travel downstream with positive characteristic velocity u_{c+} ; contrary, in cases where the traffic is congested, they propagate upstream, against the traffic flow, with characteristic velocity u_{c-} . However, according to [22], the positive characteristic velocity u_{c+} will decay to zero rapidly with time and does not play a particularly important role. Hence, in the remainder of the nonlinear stability method, we neglect the effect of the downstream moving branch of the perturbation and we concentrate on the upstream propagation with negative characteristic velocity u_{c-} .

Next, we will eliminate the second-order partial derivatives $\partial_{xx}(\rho)$ and $\partial_{xx}(u)$ in Equations (30) and (32); this is feasible by multiplying Equations (30) and (32) with the terms $\{-u_{c-}\}$ and $\left\{ \frac{1}{\rho_0} \left(\frac{1}{\tau^*} d^* u_0 - \partial_\rho(P_0) \right) \right\}$, respectively, and using properly expression (34), whereby the resulting equations are added to one another. Consequently, after some algebra, we end up with the following reduced equation

$$\dot{u}_x + a \partial_x(u) + \beta (\partial_x(u))^2 = 0, \quad (36)$$

where

$$\begin{aligned} a = 0, \\ \beta = \\ \frac{2\partial_\rho(P_0) + \rho_0 \partial_{\rho\rho}(P_0) + 2u_{c-} \partial_{\rho u}(P_0) + \frac{(u_{c-})^2}{\rho_0} \partial_{uu}(P_0) - \frac{2d^* u_0}{\tau^*} - \frac{2d^* u_{c-}}{\tau^*}}{(u_{c-})^2 + \partial_\rho(P_0) - \frac{d^* u_0}{\tau^*}} \end{aligned} \quad (37)$$

The solution of Equation (36) is given as

$$\partial_x(u(t)) = \frac{\partial_x(u(0))}{\partial_x(u(0))\beta t + 1}, \quad (38)$$

where $\partial_x(u(0))$ is the initial condition for $\partial_x(u(t))$.

According to Equation (38), the trend of $\partial_x(u(t))$ can be defined using the derivative:

$$\frac{d(\partial_x(u(t)))}{dt} = \frac{-(\partial_x(u(0)))^2 \beta}{(\partial_x(u(0))\beta t + 1)^2}. \quad (39)$$

From Equation (38), if the denominator becomes zero, then $\partial_x(u(t))$ tends to infinity and traffic becomes nonlinearly unstable; more precisely, this can happen when $\partial_x(u(0))\beta t + 1 = 0$ or when $t = -1/(\partial_x(u(0))\beta)$. As t is always positive, for the satisfaction of the previous condition we should have $\partial_x(u(0))\beta < 0$. Thus, for the unstable regions, the solution must satisfy the following two restrictions: $\{\partial_x(u(0)) < 0 \text{ and } \beta > 0\}$ or $\{\partial_x(u(0)) > 0 \text{ and } \beta < 0\}$. However, for most second-order models, $\beta > 0$ [22, 32]; thus we expect that unstable regions emerge when $\partial_x(u(0)) < 0$.

4. NUMERICAL SIMULATION

In this section, we investigate numerically the findings of the theoretical analysis, assuming the traffic flow inside a single-lane ring-road of circumference $L=10$ km; periodic boundary conditions were implemented at the boundaries of the discretized section. The second-order model is numerically approximated by an accurate and robust high-resolution finite volume relaxation scheme, where the nonlinear system of partial differential equations is first recast to a diagonalizable semi-linear system and is then discretized by a higher-order WENO scheme [25, 35].

We consider an initial perturbation of the average density, as it is depicted in Fig. 1, given as:

$$\begin{aligned} \rho = \bar{\rho} - \Delta\rho \frac{1}{2} \left[1 + \tanh\left(\frac{x-x_1}{\Delta x}\right) \right] \\ + \Delta\rho \frac{1}{2} \left[1 + \tanh\left(\frac{x-x_2}{\Delta x}\right) \right], \end{aligned} \quad (40)$$

where $\bar{\rho} = 45$ Veh/km, $\Delta\rho = 5$ veh/km, $\Delta x = 400$ m, $x_1 = 4000$ m, and $x_2 = 7000$ m. The resulting velocity perturbation

is also presented in Fig. 1. The initial perturbation was selected in order to produce the condition $\partial_x(u(0)) < 0$.

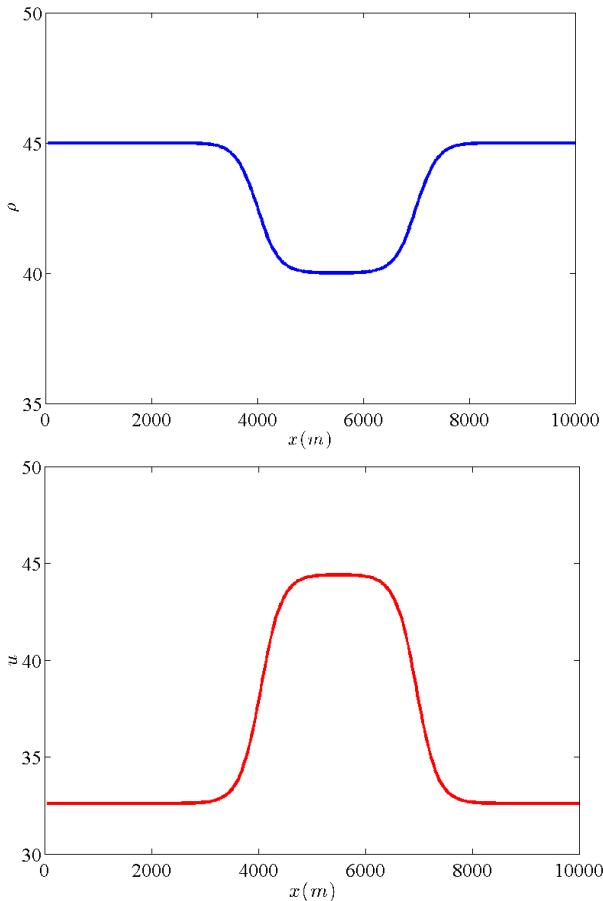


Fig. 1: The initial perturbation in ρ (top) and u (bottom), applied for the numerical example.

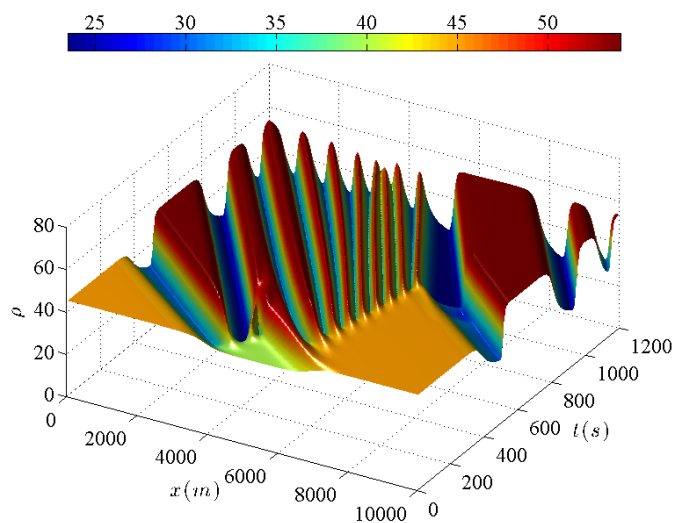


Fig. 2: Density evolution for manually driven cars.

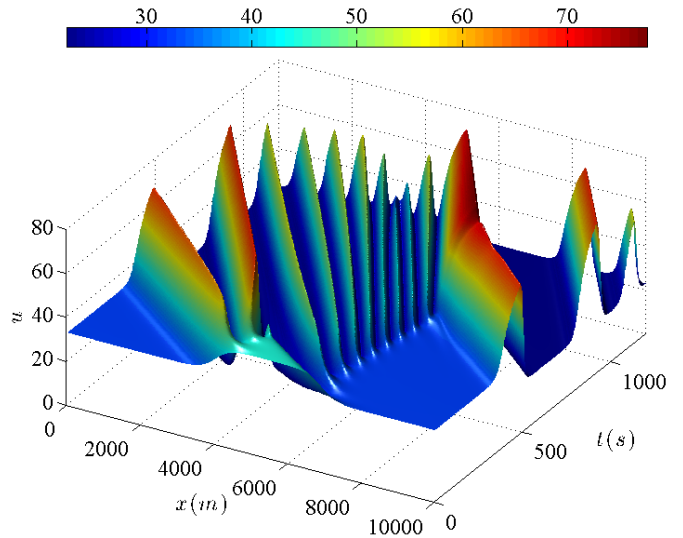


Fig. 3: Velocity evolution for manually driven cars.

The ring was discretized with $npts = 400$ grid points, while the model parameters used in the simulation of the GKT model were $u_{max} = 110 \text{ km/h}$, $\rho_{max} = 160 \text{ veh/km}$, $\rho_{cr} = 0.27\rho_{max}$, $\tau = 35 \text{ s}$, $A_0 = 0.008$, $\delta A = 0.02$, $\delta\rho = 0.05\rho_{max}$, $T = 1.8 \text{ s}$, $\gamma = 1.2$. Simulations are reported up to 1200 s. First the manual flow was simulated (by setting $p = 0$ in Equation (2)).

The simulation results for manual cars are presented in Figs. 2 and 3 for density and velocity, respectively; a cascade of stop-and-go waves emerges from the perturbation in the initial condition.

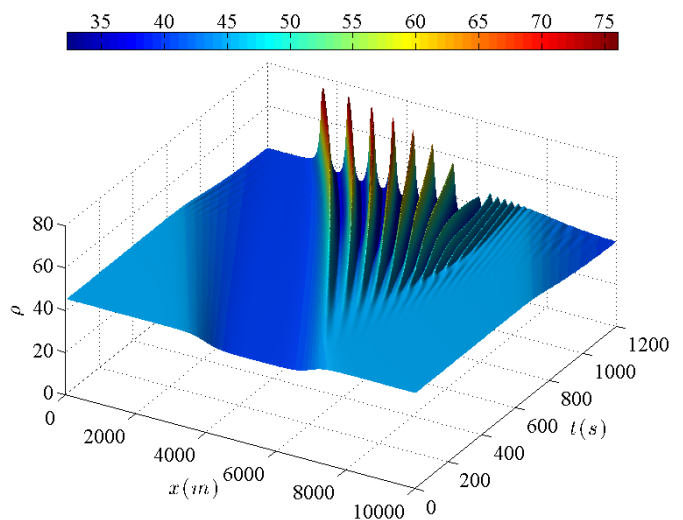


Fig. 4: Density evolution for ACC traffic.

The corresponding simulation results for ACC traffic (by setting $p = 1$ in Equation (2)) are presented in Figs. 4 and 5, for density and velocity evolution, respectively. The same initial perturbation was used as for the flow with manual vehicles. The

time gap was set equal to $T^* = 1$ s, while $\rho_{acc} = 0.9 \rho_{cr}$, $\gamma^* = 1$ and $\tau^* = 0.5$ s. As it can be observed, the original cascade of stop-and-go waves (produced in the manual traffic) has been eliminated; however, a series of growing instabilities emerges from the region where $\partial_x(u(0)) < 0$ in the initial condition. This observation is compatible with the findings of the theoretical investigation.

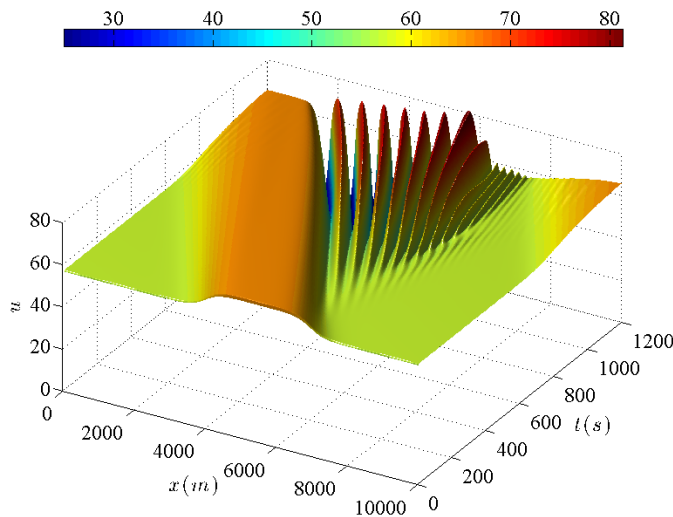


Fig. 5: Velocity evolution for ACC traffic.

5. CONCLUSIONS

In this work the wavefront expansion method, with respect to large perturbations, was applied to analytically derive the stability region of a recently introduced second-order macroscopic traffic flow model that is able to model the dynamics of ACC traffic flows. The development of the proposed model was based on the GKT one, while the modeling of ACC traffic was incorporated by adding a proper source term to the momentum equation of the original model; this additional term was developed to satisfy the time/space-gap principle of ACC systems. From the nonlinear stability analysis performed in this work, the unstable regions for ACC traffic have been derived, assuming that all the cars are equipped with ACC and the flow is in the congested region (where ACC is always activated for all cars). As it was deduced from the analysis, an unstable region emerges when $\partial_x(u(0)) < 0$ (assuming that the β parameter in Equation (36) has a positive value). The theoretical findings are supported by the simulation results derived for a numerical test in a single-lane ring-road with a perturbation in the initial conditions of density and speed. The simulation results revealed that a series of growing instabilities emerges from the region in the initial conditions where the instability criterion is valid.

On-going work includes the derivation of stability criteria for the case of ACC penetration rates lower than 1, and for the

CACC case (which can be also covered by the proposed macroscopic model [25]).

ACKNOWLEDGEMENTS

This research was supported by Traffic Management for the 21st century (TRAMAN21) ERC Advanced Investigator Grand under the European Union's Seventh Framework Programme (FP/2007-2013).

REFERENCES

- [1] Treiber, M., Hennecke, A., and Helbing, D., 2000, "Congested traffic states in empirical observations and microscopic simulations," *Phys. Rev. E*, **62**(2), pp. 1805–1824.
- [2] Kesting, A., Treiber, M., and Helbing, D., 2007, "General Lane-Changing Model MOBIL for Car-Following Models," *Transp. Res. Rec. J. Transp. Res. Board*, **1999**, pp. 86–94.
- [3] Tang, T. Q., Li, C. Y., Wu, Y. H., and Huang, H. J., 2011, "Impact of the honk effect on the stability of traffic flow," *Phys. Stat. Mech. Its Appl.*, **390**(20), pp. 3362–3368.
- [4] Ge, H.-X., Liu, Y.-X., Cheng, R.-J., and Lo, S.-M., 2012, "A modified coupled map car following model and its traffic congestion analysis," *Commun. Nonlinear Sci. Numer. Simul.*, **17**(11), pp. 4439–4445.
- [5] Zhang, P., and Wong, S. C., 2006, "Essence of conservation forms in the traveling wave solutions of higher-order traffic flow models," *Phys. Rev. E Stat. Nonlin. Soft Matter Phys.*, **74**(2 Pt 2), p. 026109.
- [6] Gupta, A. K., and Katiyar, V. K., 2007, "A New Multi-Class Continuum Model for Traffic Flow," *Transportmetrica*, **3**(1), pp. 73–85.
- [7] Tang, T. Q., Huang, H. J., and Xu, G., 2008, "A new macro model with consideration of the traffic interruption probability," *Phys. Stat. Mech. Its Appl.*, **387**(27), pp. 6845–6856.
- [8] Zhang, P., Wong, S. C., and Dai, S. Q., 2009, "A conserved higher-order anisotropic traffic flow model: Description of equilibrium and non-equilibrium flows," *Transp. Res. Part B Methodol.*, **43**(5), pp. 562–574.
- [9] Davis, L. C., 2004, "Effect of adaptive cruise control systems on traffic flow," *Phys. Rev. E*, **69**(6).
- [10] Davis, L. C., 2007, "Effect of adaptive cruise control systems on mixed traffic flow near an on-ramp," *Phys. Stat. Mech. Its Appl.*, **379**(1), pp. 274–290.
- [11] Kesting, A., Treiber, M., Schönhof, M., Kranke, F., and Helbing, D., 2007, "Jam-Avoiding Adaptive Cruise Control (ACC) and its Impact on Traffic Dynamics," *Traffic and Granular Flow'05*, A. Schadschneider, T. Pöschel, R. Kühne, M. Schreckenberg, and D.E. Wolf, eds., Springer Berlin Heidelberg, pp. 633–643.
- [12] Kesting, A., Treiber, M., Schönhof, M., and Helbing, D., 2008, "Adaptive cruise control design for active congestion avoidance," *Transp. Res. Part C Emerg. Technol.*, **16**(6), pp. 668–683.
- [13] Kesting, A., Treiber, M., and Helbing, D., 2010, "Enhanced Intelligent Driver Model to Access the Impact of Driving Strategies on Traffic Capacity," *Philos. Trans. R. Soc. Math. Phys. Eng. Sci.*, **368**(1928), pp. 4585–4605.

- [14] Ntousakis, I. A., Nikolos, I. K., and Papageorgiou, M., 2014, "On microscopic modeling of Adaptive Cruise Control systems," Proc. 4th International Symposium of Transport Simulation, Corsica, France.
- [15] Swaroop, D., Hedrick, J. K., Chien, C. C., and Ioannou, P., 1994, "A Comparison of Spacing and Headway Control Laws for Automatically Controlled Vehicles¹," Veh. Syst. Dyn., **23**(1), pp. 597–625.
- [16] Swaroop, D., and Hedrick, J. K., 1996, "String stability of interconnected systems," IEEE Trans. Autom. Control, **41**(3), pp. 349–357.
- [17] Liang, C.-Y., and Peng, H., 2000, "String Stability Analysis of Adaptive Cruise Controlled Vehicles," JSME Int. J. Ser. C, **43**(3), pp. 671–677.
- [18] Li, P. Y., and Shrivastava, A., 2002, "Traffic flow stability induced by constant time headway policy for adaptive cruise control vehicles," Transp. Res. Part C Emerg. Technol., **10**(4), pp. 275–301.
- [19] Yi, J., and Horowitz, R., 2006, "Macroscopic traffic flow propagation stability for adaptive cruise controlled vehicles," Transp. Res. Part C Emerg. Technol., **14**(2), pp. 81–95.
- [20] Swaroop, D., and Rajagopal, K. R., 1999, "Intelligent cruise control systems and traffic flow stability," Transp. Res. Part C Emerg. Technol., **7**(6), pp. 329–352.
- [21] Demir, C., 2003, "Modelling the Impact of ACC-Systems on the Traffic Flow at Macroscopic Modelling Level," Traffic and Granular Flow'01, M. Fukui, Y. Sugiyama, M. Schreckenberg, and D.E. Wolf, eds., Springer Berlin Heidelberg, pp. 305–317.
- [22] Yi, J., Lin, H., Alvarez, L., and Horowitz, R., 2003, "Stability of macroscopic traffic flow modeling through wavefront expansion," Transp. Res. Part B Methodol., **37**(7), pp. 661–679.
- [23] Ngoduy, D., 2012, "Application of gas-kinetic theory to modelling mixed traffic of manual and ACC vehicles," Transportmetrica, **8**(1), pp. 43–60.
- [24] Treiber, M., and Kesting, A., 2013, Traffic Flow Dynamics: Data, Models and Simulation, Springer Berlin Heidelberg.
- [25] Delis, A. I., Nikolos, I. K., and Papageorgiou, M., 2015, "Macroscopic traffic flow modeling with adaptive cruise control: Development and numerical solution," Comput. Math. Appl., **70**(8), pp. 1921–1947.
- [26] Prigogine, I., and Andrews, F. C., 1960, "A Boltzmann-Like Approach for Traffic Flow," Oper. Res., **8**(6), pp. 789–797.
- [27] Helbing, D., 1997, "Modeling multi-lane traffic flow with queuing effects," Phys. Stat. Mech. Its Appl., **242**(1–2), pp. 175–194.
- [28] Treiber, M., Hennecke, A., and Helbing, D., 1999, "Derivation, properties, and simulation of a gas-kinetic-based, nonlocal traffic model," Phys. Rev. E, **59**(1), pp. 239–253.
- [29] Helbing, D., Hennecke, A., Shvetsov, V., and Treiber, M., 2001, "MASTER: macroscopic traffic simulation based on a gas-kinetic, non-local traffic model," Transp. Res. Part B Methodol., **35**(2), pp. 183–211.
- [30] Ngoduy, D., 2013, "Platoon-based macroscopic model for intelligent traffic flow," Transp. B Transp. Dyn., **1**(2), pp. 153–169.
- [31] Ngoduy, D., and Tampere, C., 2009, "Macroscopic effects of reaction time on traffic flow characteristics," Phys. Scr., **80**(2).
- [32] Ngoduy, D., 2013, "Instability of cooperative adaptive cruise control traffic flow: A macroscopic approach," Commun. Nonlinear Sci. Numer. Simul., **18**(10), pp. 2838–2851.
- [33] Ngoduy, D., 2006, "Derivation of Continuum Traffic Model for Weaving Sections on Freeways," Transportmetrica, **2**(3), pp. 199–222.
- [34] Ngoduy, D., Hoogendoorn, S. P., and Liu, R., 2009, "Continuum modeling of cooperative traffic flow dynamics," Phys. Stat. Mech. Its Appl., **388**(13), pp. 2705–2716.
- [35] Delis, A. I., Nikolos, I. K., and Papageorgiou, M., 2014, "High-resolution numerical relaxation approximations to second-order macroscopic traffic flow models," Transp. Res. Part C Emerg. Technol., **44**, pp. 318–349.
- [36] Helbing, D., and Treiber, M., 1998, "Gas-Kinetic-Based Traffic Model Explaining Observed Hysteretic Phase Transition," Phys. Rev. Lett., **81**(14), pp. 3042–3045.
- [37] Treiber, M., and Helbing, D., 1999, "Macroscopic simulation of widely scattered synchronized traffic states," J. Phys. Math. Gen., **32**(1), pp. L17-L23.
- [38] Shladover, S., Su, D., and Lu, X.-Y., 2012, "Impacts of Cooperative Adaptive Cruise Control on Freeway Traffic Flow," Transp. Res. Rec. J. Transp. Res. Board, **2324**, pp. 63–70.
- [39] Zhou, J., and Peng, H., 2005, "Range policy of adaptive cruise control vehicles for improved flow stability and string stability," IEEE Trans. Intell. Transp. Syst., **6**(2), pp. 229–237.
- [40] Treiber, M., and Kesting, A., 2011, "Evidence of convective instability in congested traffic flow: A systematic empirical and theoretical investigation," Transp. Res. Part B Methodol., **45**(9), pp. 1362–1377.
- [41] Helbing, D., and Johansson, A., 2009, "On the Controversy around Daganzo's Requiem for and Aw-Rascle's Resurrection of Second-Order Traffic Flow Models," Eur. Phys. J. B, **69**(4), pp. 549–562.
- [42] Ngoduy, D., 2012, "Effect of driver behaviours on the formation and dissipation of traffic flow instabilities," Nonlinear Dyn., **69**(3), pp. 969–975.
- [43] Ngoduy, D., 2014, "Generalized macroscopic traffic model with time delay," Nonlinear Dyn., **77**(1-2), pp. 289–296.
- [44] Porfyri, K.N., Nikolos, I.K., Delis, A.I., Papageorgiou, M., 2015, "Stability analysis of a macroscopic traffic flow model for adaptive cruise control systems," Proc. of the International Mechanical Engineering Congress and Exposition IMECE 2015, Houston, Texas, USA, **15**, Paper No. IMECE2015-50977.
- [45] Whitham, G. B., 1974, Linear and Nonlinear Waves, John Wiley & Sons.